6th European Conference on Computational Mechanics (ECCM 6)
7th European Conference on Computational Fluid Dynamics (ECFD 7)
1115 June 2018, Glasgow, UK

NUMERICAL SIMULATION OF A LIQUID SODIUM TURBULENT FLOW OVER A BACKWARD FACING STEP WITH A FOUR PARAMETER LOGARITHMIC TURBULENCE MODEL

R. Da Vià[1,*], A. Chierici[2,*], L. Chirco[3,*] and S. Manservisi[4,*]

[*] University of Bologna, via dei Colli 16, 40136, Bologna, Italy; [1]roberto.davia2@unibo.it, [2]andrea.chierici4@unibo.it, [3]leonardo.chirco2@unibo.it, [4]sandro.manservisi@unibo.it.

Key words: Liquid Metals, Mixed Convection, Buoyancy, Four parameter turbulence model

Abstract. In recent years a great interest has grown around liquid metals. These fluids are characterized by much higher thermal conductivity, if compared with standard fluids like air and water and can be used in applications where large heat fluxes are present while being subjected to small temperature gradients. In the present paper we simulate a turbulent flow of liquid sodium, with a Prandtl number equal to 0.0088, over a vertical backward-facing step. A uniform heat flux is applied on the vertical wall next to the change of cross section. Reynolds stresses and turbulent heat flux are modeled with a four logarithmic parameter turbulence model. We investigate the cases of purely forced convection, where the temperature field is just a passive scalar, and of mixed convection, where temperature has an impact on the fluid behavior through a buoyancy term that is introduced in the momentum equation with the Boussinesq approximation. The results are reported for various values of the Richardson number, i.e. Ri=0 for the purely forced convection and Ri>0 for the mixed convection case, and compared with data coming from Direct Numerical Simulations that are available in literature.

1 INTRODUCTION

Liquid metals are becoming an interesting type of fluids for engineering applications [1]. From the physical properties point of view these fluids have low viscosity and high thermal diffusivity, which lead to values of molecular Prandtl number much smaller than one. At ambient pressure lead, bismuth, sodium and lithium can be kept in liquid phase on a wide temperature range. This characteristic allows scientists and engineers to use liquid metals in applications where huge amounts of heat transfer occur without the need of using pressurized systems. As pointed out in numerous works, from the computational point of view, different and more sophisticated means are required in order to accurately simulate turbulent heat transfer involving liquid metals [2, 3, 4]. Direct Numerical Simulation (DNS) have been performed with the purpose of providing reference data to be used for

evaluating the accuracy of turbulence models [5]. Four parameter turbulence models have been developed for the evaluation of thermal field characteristic time scales [6, 7, 8]. Other turbulence models have been developed to obtain increased numerical stability [9] or to propose more sophisticated expressions of turbulent heat flux, in order to take into account flow anisotropic behavior [10].

With the present paper we deal with the simulation of a liquid sodium turbulent flow over a backward facing step. This is a geometry that has been extensively studied by many researchers, from the kinematic point of view, as it is a geometry configuration that can be found in many engineering applications. Many works have recently been proposed to investigate the behavior of liquid sodium turbulent flow over such geometry, in particular to study the influence of buoyancy on the flow pattern for mixed convection cases. The flow regime will be denoted through the value of the Richardson number Ri which is defined as $Ri = g\beta\Delta T h/U_b^2$ where g is the modulus of gravity acceleration, β the thermal expansion coefficient, ΔT a reference temperature difference, h the step height and U_b the bulk velocity. We here report a brief review on the known literature studies for this type of flow. A first DNS simulation for a liquid sodium turbulent flow over a backward facing step, with $Ri = 0$, is provided in [11], for a particular geometry where a constant heat flux is applied on the whole wall behind the step. For the same simulation case, i.e. geometry configuration and Reynolds number Re, other studies are performed [12, 13]. In [12] a comparison is provided between the results obtained from DNS simulation and from the solution of a Reynolds Averaged Navier Stokes (RANS) system of equations closed with various turbulence models. The considered case is of pure forced convection. It is shown that two equation heat transfer turbulence models, coupled with non linear expressions for Reynolds stresses, allow to improve the predictions of heat flux within the re-circulation zone. In [13] a DNS study is performed for the cases $Ri = 0$ and $Ri = 0.338$. In particular, for the mixed convection case, i.e. $Ri = 0.338$, a different domain configuration is considered as an adiabatic section is added behind the heated wall in order to minimize the influence of the outlet on the flow behavior over the heated wall. Here the effect of buoyancy results in a diminished recirculation length with respect to the case of pure forced convection. A great number of simulations have been performed for studying the influence of buoyancy for a liquid sodium turbulent flow with $Re = 10000$ [14, 15, 16, 17, 18]. Various Richardson number cases are simulated, ranging from $Ri = 0$ to $Ri = 1$. In [14, 15, 16] DNS simulations are performed for various values of the Richardson number, showing that recirculation length decreases and heat transfer increases within the recirculation zone as Ri increases. These studies provide useful data for the evaluation of turbulence models. In [16] Large Eddy Simulations (LES) are performed for higher Reynolds numbers, namely $Re_h = 20000$ and $Re_h = 40000$. Numerical simulations with RANS models are reported in [17, 18]. In the first work a comparison is performed between the results obtained using a four parameter turbulence model [8, 19, 20, 21] and a two equation turbulence model [22], for modeling the Reynolds stresses, and the Kays correlation for modeling the eddy thermal diffusivity [23]. It is shown that similar results are obtained using the two different models, for that particular Reynolds number case. In the latter work a study on a wider range of

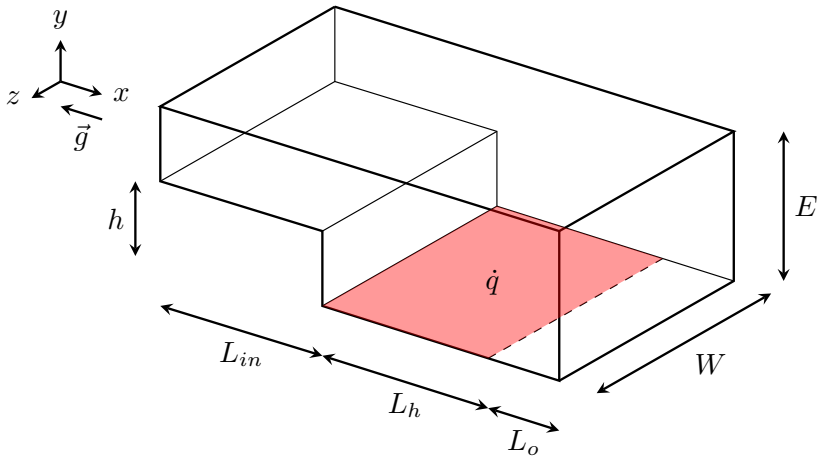

Figure 1: Sketch of backward facing step geometry.

Richardon number values is performed. Here the RANS system of equation is closed by using a two equation model and the Kays correlation. A comparison between the previously mentioned literature data is reported in Table 1, where the backward facing step geometry is parametrized by using the step height h and the length labels for inlet section L_{in}, heated section L_h, adiabatic section L_a, domain width W and downstream channel height E, as sketched in Fig. 1. We refer to E_r as the expansion ratio, calculated as $E_r = E/(E-h)$.

Table 1: Comparison of literature studies on sodium buoyant turbulent flows on backward facing step, as a function of geometrical parameters and of Reynolds and Richardson numbers.

	L_{in}/h	L_h/h	L_a/h	E_r	W/h	Re_h	Method	Ri
[11]	2	20	0	1.5	4	4805	DNS	0
[12]	2	20	0	1.5	4	4805	DNS/RANS	0
[13]	2	20	10	1.5	4	4805	DNS	0 - 0.338
[14]	2	20	10	2	4	10000	DNS	0 - 0.12 - 0.2
[15]	2	20	10	2	4	10000	DNS	0 - 0.12 - 0.2 - 0.4
[16]	2	20	10	2	1	10000 20000 40000	DNS LES LES	0 - 0.2
[17]	4	20	20	2	-	10000	RANS	0 - 0.2
[18]	4	20	20	2	-	10000	RANS	0 - 0.12 - 0.2 - 0.4 - 1

2 NUMERICAL METHOD

The liquid sodium turbulent flow over a backward facing step is simulated using a RANS set of equations. We use the assumptions of incompressible flow and the Boussinesq approximation in order to account for buoyancy forces. The system of equations consists

then of the following

$$\boldsymbol{\nabla}\cdot\mathbf{u}=0\,, \tag{1}$$

$$\frac{\partial\mathbf{u}}{\partial t}+(\mathbf{u}\cdot\boldsymbol{\nabla})\mathbf{u}=-\frac{1}{\rho}\boldsymbol{\nabla}P+\boldsymbol{\nabla}\cdot\left[\nu\left(\boldsymbol{\nabla}\mathbf{u}+\boldsymbol{\nabla}\mathbf{u}^{T}\right)-\overline{\mathbf{u}'\mathbf{u}'}\right]-\mathbf{g}\beta(T-T_{in})\,, \tag{2}$$

$$\frac{\partial T}{\partial t}+\mathbf{u}\cdot\boldsymbol{\nabla}T=\boldsymbol{\nabla}\cdot\left[\alpha\boldsymbol{\nabla}T-\overline{\mathbf{u}'T'}\right]\,, \tag{3}$$

where $\mathbf{u}$, P and T are the mean velocity, pressure and temperature. The unknown Reynolds stresses $\rho\overline{\mathbf{u}'\mathbf{u}'}$ and the turbulent heat flux $\rho C_p\overline{\mathbf{u}'T'}$ are modeled with the following logarithmic four parameter turbulence model

$$\frac{\partial \mathrm{K}}{\partial t}+\mathbf{u}\cdot\boldsymbol{\nabla}\mathrm{K}=\boldsymbol{\nabla}\cdot\left[\left(\nu+\frac{\nu_t}{\sigma_k}\right)\boldsymbol{\nabla}\mathrm{K}\right]+\left(\nu+\frac{\nu_t}{\sigma_\varepsilon}\right)\boldsymbol{\nabla}\mathrm{K}\cdot\boldsymbol{\nabla}\mathrm{K}+\frac{P_k}{e^{\mathrm{K}}}-C_\mu\, e^{\Omega}\,, \tag{4}$$

$$\begin{aligned}\frac{\partial \Omega}{\partial t}+\mathbf{u}\cdot\boldsymbol{\nabla}\Omega=&\boldsymbol{\nabla}\cdot\left[\left(\nu+\frac{\nu_t}{\sigma_\varepsilon}\right)\boldsymbol{\nabla}\Omega\right]+2\left(\nu+\frac{\nu_t}{\sigma_\varepsilon}\right)\boldsymbol{\nabla}\mathrm{K}\cdot\boldsymbol{\nabla}\Omega+\\&+\left(\nu+\frac{\nu_t}{\sigma_\varepsilon}\right)\boldsymbol{\nabla}\Omega\cdot\boldsymbol{\nabla}\Omega+\frac{c_{\varepsilon 1}-1}{e^{\mathrm{K}}}P_k-C_\mu\left(c_{\varepsilon 2}f_{exp}-1\right)e^{\Omega}\end{aligned} \tag{5}$$

$$\frac{\partial \mathrm{K}_\theta}{\partial t}+\mathbf{u}\cdot\boldsymbol{\nabla}\mathrm{K}_\theta=\boldsymbol{\nabla}\cdot\left[\left(\alpha+\frac{\alpha_t}{\sigma_\theta}\right)\boldsymbol{\nabla}\mathrm{K}_\theta\right]+\left(\alpha+\frac{\alpha_t}{\sigma_\theta}\right)\boldsymbol{\nabla}\mathrm{K}_\theta\cdot\boldsymbol{\nabla}\mathrm{K}_\theta+\frac{P_\theta}{e^{\mathrm{K}_\theta}}-C_\mu\, e^{\Omega_\theta}\,, \tag{6}$$

$$\begin{aligned}\frac{\partial \Omega_\theta}{\partial t}+\mathbf{u}\cdot\boldsymbol{\nabla}\Omega_\theta=&\boldsymbol{\nabla}\cdot\left[\left(\alpha+\frac{\alpha_t}{\sigma_{\varepsilon_\theta}}\right)\boldsymbol{\nabla}\Omega_\theta\right]+2\left(\alpha+\frac{\alpha_t}{\sigma_{\varepsilon_\theta}}\right)\boldsymbol{\nabla}\mathrm{K}_\theta\cdot\boldsymbol{\nabla}\Omega_\theta+\\&+\left(\alpha+\frac{\alpha_t}{\sigma_{\varepsilon_\theta}}\right)\boldsymbol{\nabla}\Omega_\theta\cdot\boldsymbol{\nabla}\Omega_\theta+\frac{c_{p1}-1}{e^{\mathrm{K}_\theta}}P_\theta+\frac{c_{p2}}{e^{\mathrm{K}}}P_k-\left(c_{d1}-1\right)C_\mu e^{\Omega_\theta}-c_{d2}C_\mu e^{\Omega}\,.\end{aligned} \tag{7}$$

The model is a full logarithmic version of the one reported in [9]. The state variables, namely K, Ω, K_θ and Ω_θ, represent the logarithmic values of turbulent kinetic energy k and its specific dissipation ω, mean squared temperature fluctuations k_θ and their specific dissipation rate ω_θ. The interested reader can find the definition of model constants and functions in [9] . The model has been obtained to provide an increased numerical stability with respect to the original formulation. The system of equations is solved with a finite element code on a domain discretization having a non dimensional wall normal distance $y^+=\delta u_\tau/\nu$ smaller than five on the first mesh point near wall boundaries, where δ is the wall distance, u_τ the friction velocity and ν the fluid kinematic viscosity.

3 RESULTS

Table 2: Non-dimensional parameters for the classification of the studied case.

L_{in}/h	L_h/h	L_a/h	E_r	W/h	Re_h	Method	Ri
2	20	0	1.5	0	4805	RANS	0 - 0.338

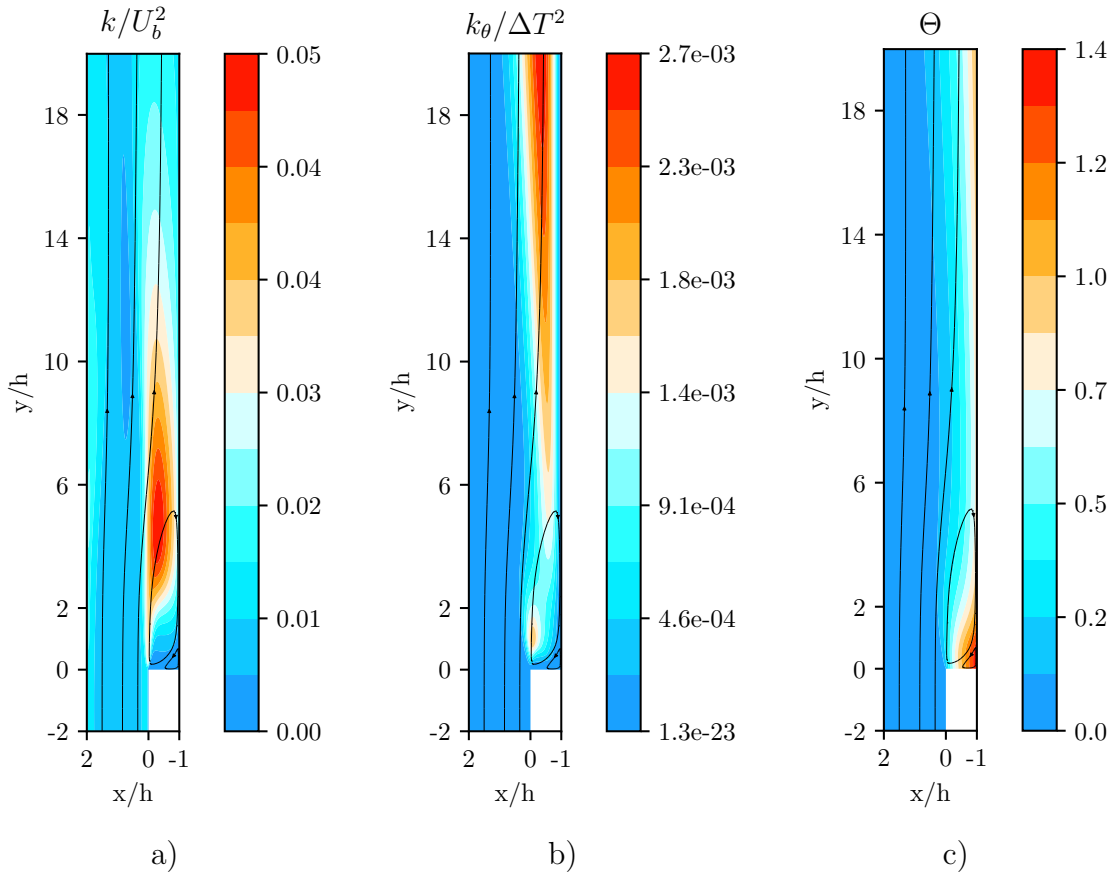

Figure 2: Non-dimensional values of mean squared velocity fluctuations a), mean squared temperature fluctuations b) and temperature difference c) for the case of Richardon number equal to 0.

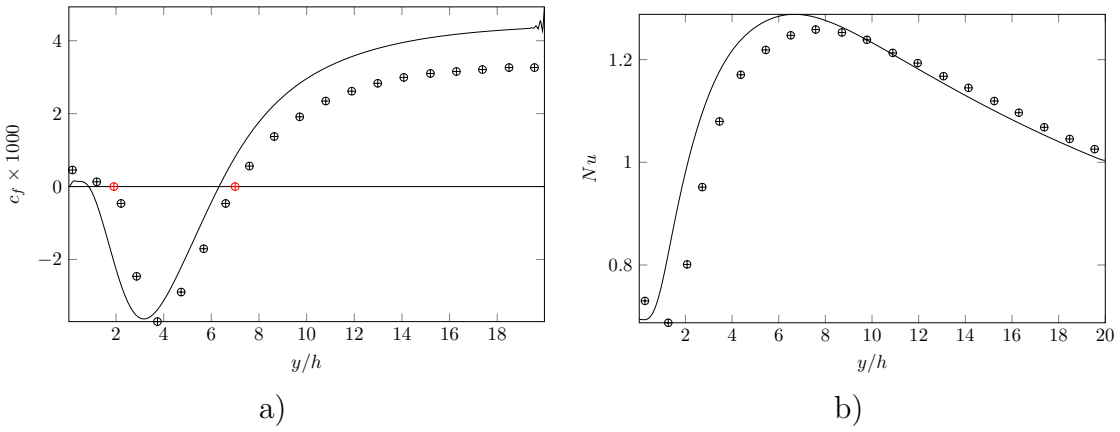

Figure 3: Skin friction coefficient c_f a) and Nusselt number values b) along the heated wall. The results are compared with DNS data obtained from [13].

In the present work we report the results obtained for the simulation of a backward facing step case similar to those studied in [11, 12, 13]. The geometrical parameters of the simulated domain are reported in Table 2, in accordance with the classification proposed

in Table 1. On the inlet section of the domain we impose a velocity field obtained from the simulation of a fully developed turbulent channel flow having a friction Reynolds number $Re_\tau \simeq 300$. The obtained mean velocity leads to a Reynolds number $Re_h = 4805$. Homogeneous Neumann boundary conditions are imposed on the inlet section for the resolved turbulence variables, while for temperature a uniform value equal to 150°C is set. The same temperature is used as reference temperature for the evaluation of the liquid sodium physical properties used in the system (1 - 7) through the correlations provided in [24]. We obtain a molecular Prandtl number equal to $Pr = 0.0088$. On the wall boundaries we impose no slip boundary condition for the velocity field, adiabatic boundary condition for the temperature field with the exception of the wall behind the step where a uniform heat flux $\dot{q}$ is imposed. For the turbulence variables we use boundary conditions in accordance with their near wall behavior. On the outlet section an outflow boundary condition is imposed on the velocity field, while for all the other variables we set a zero gradient. We study the cases of pure forced convection, i.e. $Ri = 0$ by setting $\beta = 0$, and the mixed convection case for $Ri = 0.338$ in order to compare the results with the ones obtained in [12, 13].

Case $Ri = 0$ A view of the non-dimensional turbulent kinetic energy is reported in Fig. 2 a), where the field is calculated as k/U_b^2, being U_b the bulk velocity on the inlet section. In the same Fig. the flow streamlines are presented, showing the presence of the two typical vortices that arise behind the step. The turbulent kinetic energy reaches its maximum value in the region near the reattaching point and then decreases in stream-wise direction. On the contrary the mean squared temperature fluctuations behave, as can be seen in Fig. 2 b). The skin friction $c_f = 2\tau_w/\rho U_b^2$ profile along the heated wall is shown in Fig. 3 a) and compared with DNS values obtained from the profile presented in [13]. By seeing the change of sign in the values of c_f we can calculate the reattaching lengths of the two vortices that are present in the region behind the step. In particular, in terms of non-dimensional stream-wise coordinate $\tilde{y} = y/h$ with $\tilde{y} = 0$ being the position of the step, we obtain the values $\tilde{y}_1 \simeq 0.85$ and $\tilde{y}_2 \simeq 6.32$. The reattaching positions obtained from DNS calculation are reported with red color in Fig. 3 a). As observed in [12] the model underestimates the corner eddy and the reattachment lengths. A better agreement with DNS results is obtained for the Nusselt number values, in particular in the region behind the reattachment point, as can be seen in Fig. 3 b), while for $\tilde{y} < 7$ the Nusselt number values are overestimated by the four parameter turbulence model. The Nusselt number is here calculated as $Nu = \dot{q}h/(T - T_{in})\lambda$, where λ is the liquid sodium thermal conductivity calculated for $T = 150$°C. The effects of reattachment lengths underestimation is reflected in the values of non dimensional temperature increment Θ, calculated as $\Theta = (T - T_{in})/\Delta T$. The values of Θ field are reported in Fig. 2 c). Maximum and minimum values of Θ, together with their position, along the heated wall are reported in Table 3 and compared with the relative DNS data. The maximum value of Θ is obtained in the recirculation area and it is close to the DNS value, while its position is shifted in upstream direction due to the underestimation of the smaller eddy reattachment point. The wall temperature value then increases in streamwise direction after the bigger

Table 3: Non dimensional temperature difference along heated wall. Maximum and minimum values, together with relative position, are compared with DNS data.

Ri		$max(\Theta_w)$		$min(\Theta_w)$	
		val	y/h	val	y/h
0	RANS	1.44	0.22	0.78	6.68
	DNS	1.45	1.01	0.79	7.32

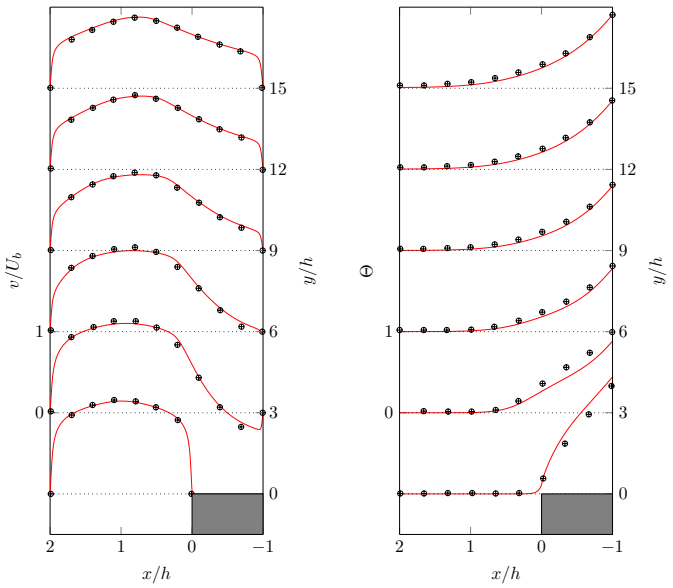

Figure 4: Non-dimensional velocity a) and temperature b) profiles on transverse channel section at various non-dimensional positions y/h. The results are for $Ri = 0$ and compared with DNS data from [13].

eddy reattachment point, showing a linear behavior. A more detailed comparison of the results with reference DNS data is given in Fig. 4 where non-dimensional profiles of velocity and temperature increment, taken on channel cross section planes, are reported for various values of streamwise direction y/h. We can observe an overall good agreement with reference data, with the exception of the temperature profiles taken on $y/h = 0$ and $y/h = 3$, which suffer from the underestimation of vortex dimensions.

Case $Ri = 0.338$ With the presence of a buoyancy force the flow field is subjected to some significant changes, as can be noted from the non-dimensional field of streamwise velocity component v/U_b that is reported in Fig. 5 a). The recirculation zone behind the step is smaller than the case of pure forced convection and the clockwise rotating vortex is now detached from the wall. We observe no reattaching point on the heated wall. The streamwise velocity component is greatly accelerated by the buoyancy force near the heated wall. The maximum temperature increment is still found in the recirculation

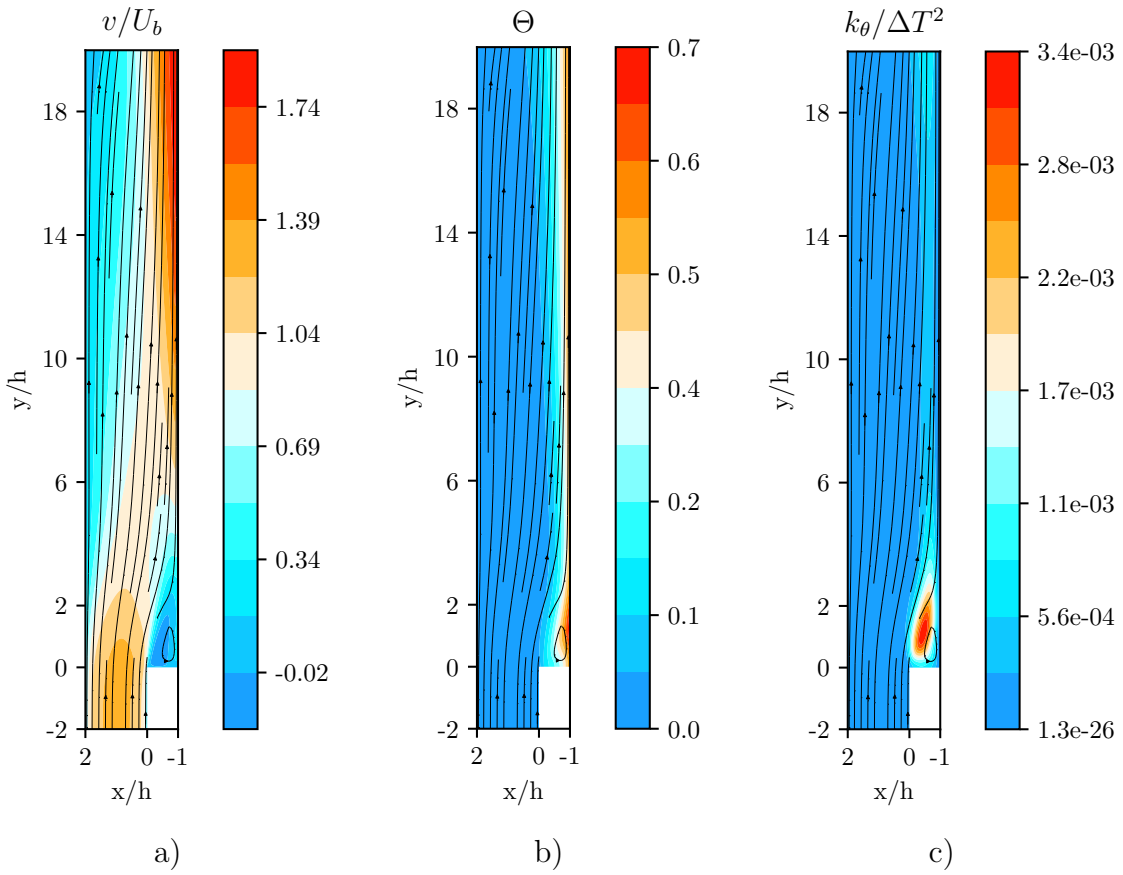

Figure 5: Non-dimensional values of streamwise velocity component a), temperature difference b) and mean squared temperature fluctuations c) for the case of Richardon number equal to 0.338.

zone, as can be seen from Fig. 5 b), but its maximum value is much smaller than this considered for $Ri = 0$. Differently from the case $Ri = 0$ the maximum value of temperature fluctuations is reached in the recirculation area, as shown in Fig. 5 c). The comparison with DNS data shows that the velocity profile, near the hot wall, is slightly underestimated, while a slight overestimation is found near the adiabatic wall, as can be seen in Fig. 6 a), where non-dimensional velocity component v/U_b profiles on cross-section planes are reported for various values of the non-dimensional position y/h. We note that there is a good matching with the location of the maximum values of v/U_b. The non-dimensional temperature gain, presented in Fig. 6 b), is very close to the reference data, so the underestimation of streamwise velocity component is not due to the buoyancy force. In Fig. 6 c) the non-dimensional turbulent kinetic energy k/U_b^2 is compared with DNS data. The biggest differences between the values computed here and the reference ones are found in the recirculation region, where an underestimation of k is present near both adiabatic and heated walls. For increasing values of the streamwise coordinate y we observe a better agreement with the DNS data. The underprediction of streamwise velocity component maximum value near the hot wall is reflected in the profile of the skin friction coefficient, along the heated wall, which is reported in Fig. 7 a), as a function

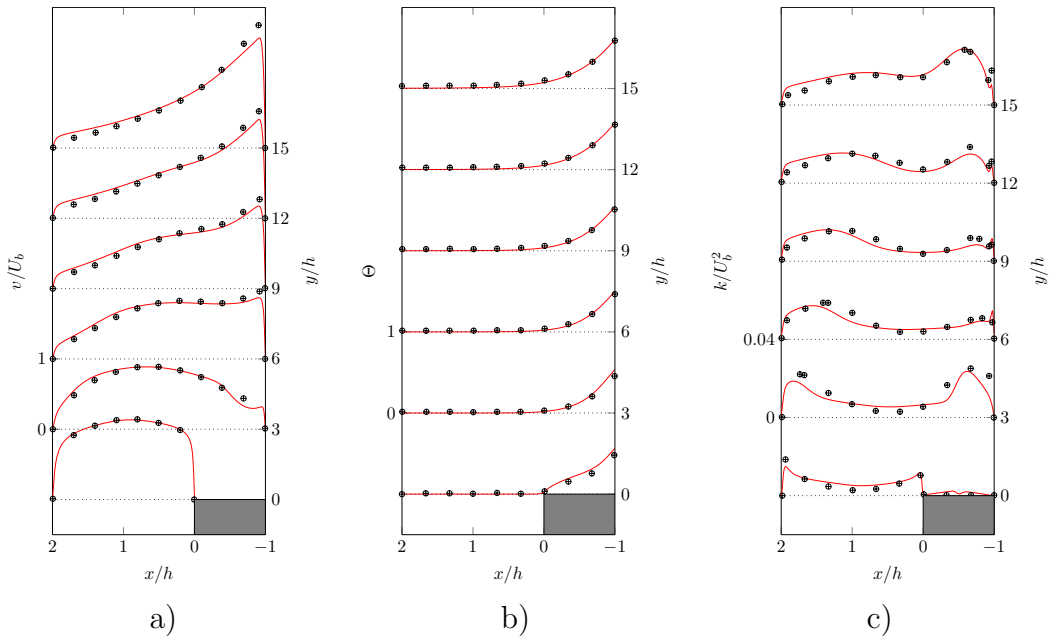

Figure 6: Non-dimensional velocity a) temperature b) and turbulent kinetic energy c) profiles on transverse channel section at various non-dimensional positions y/h. The results are for $Ri = 0.338$ and compared with DNS data from [13].

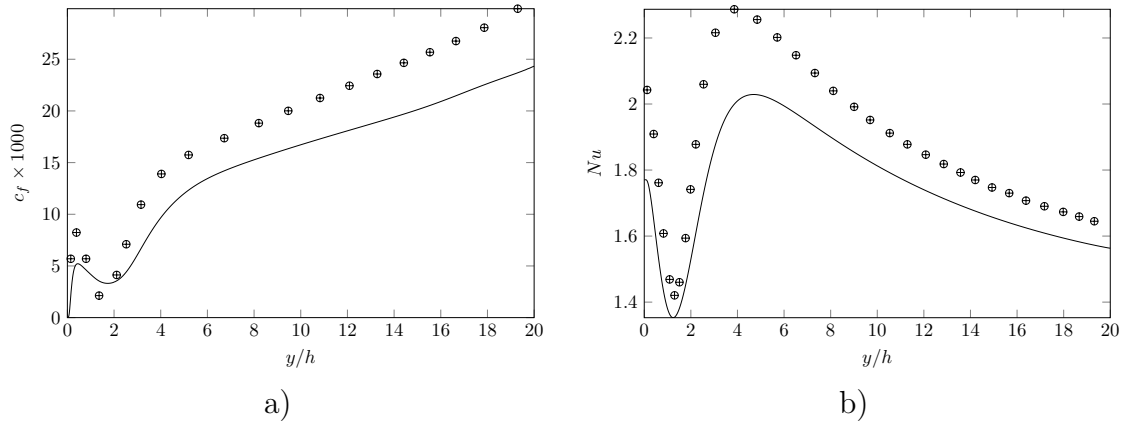

Figure 7: Skin friction coefficient c_f a) and Nusselt number values b) along the heated wall for the case $Ri = 0.338$. The results are compared with DNS data obtained from [13].

of non dimensional position y/h, and compared with DNS data from [13]. Since the skin friction coefficient c_f is proportional to the streamwise velocity component derivative along the direction normal to the wall, if the maximum value of v is smaller than the DNS one then its derivative $\partial v/\partial x$ will consecutively be smaller than the one obtained from DNS computations. We can see in Fig. 7 a) that the c_f profile shows the same qualitative behavior as the reference one, but with small values. As already mentioned, the skin friction coefficient, for this mixed convection case, does not change sign and is always positive, showing the presence of no reattaching points. In Fig. 7 b) the Nusselt

number computed on the heated wall is presented and compared with DNS data. We note a quite good agreement in the prediction of the locations of the points with Nu maximum and minimum values, while the obtained ones are generally smaller than the reference ones.

4 CONCLUSIONS

In recent years many studies have been performed with the intent to provide reference solutions for the numerical simulations of low Prandtl number fluids like liquid metals. In particular results from Direct Numerical Simulations of low Pr number fluid turbulent flows are now available in literature and they involve many geometries like plane channel, circular annulus and backward facing step. In the present work we simulated a turbulent flow of liquid sodium, having a Prandtl number equal to 0.0088, over a backward facing step with an expansion ratio $E_r = 1.5$, by using a four parameter logarithmic turbulence model. A constant heat flux is applied on the wall behind the step. We investigated a turbulent flow having a Reynolds number equal to $Re = 4805$ in both the regimes of forced and mixed convection, namely with a Richardson number $Ri = 0$ and $Ri = 0.338$. The obtained results are compared with DNS data representative of the same simulated cases, showing an overall good agreement. For the case of forced convection, as already found from other literature studies, the used turbulence model underestimate the sizes of the two vortices that arise behind the step, while a good agreement with the DNS results is found further downstream after the recirculation zone. For the mixed convection case the main discrepancies with reference results are found in a slightly difference of streamwise velocity component maximum values near the heated wall, leading to a underestimation of the skin friction coefficient on the same geometry side. Future studies will be performed dealing with a wider range of both Richardson and Reynolds numbers, in order to improve the turbulence model range of validity.

REFERENCES

[1] Heinzel A *et al.* 2017 *Energy Technol* **5** 1026–1036

[2] Cheng X and Tak N i 2006 *Nucl. Eng. Des.* **236** 385–393

[3] Cheng X and Tak N 2006 *Nucl. Eng. Des.* **236** 1874–1885

[4] Grötzbach G 2013 *Nucl. Eng. Des.* **264** 41–55

[5] Kawamura H, Abe H and Matsuo Y 1999 *Int J. Heat Fluid Fl.* **20** 196–207

[6] Nagano Y and Shimada M 1996 *Phys. Fluids* **8** 3379–3402

[7] Abe K, Kondoh T and Nagano Y 1995 *Int. J. Heat Mass Tran.* **38** 1467–1481

[8] Manservisi S and Menghini F 2014 *Int. J. Heat Mass Tran.* **69** 312–326

[9] Da Vià R, Manservisi S and Menghini F 2016 *Int. J. Heat Mass Tran.* **101** 1030–1041

[10] Hattori H, Morita A and Nagano Y 2006 *Int J. Heat Fluid Fl.* **27** 671–683

[11] Niemann M and Fröhlich J 2014 *Proc. Appl. Math. Mech* **14** 659–660

[12] Schumm T, Niemann M, Magagnato F, Marocco L, Frohnapfel B and Fr J 2015 1–12

[13] Niemann M and Fröhlich J 2016 *Int. J. Heat Mass Tran.* **101** 1237–1250

[14] Niemann M and Fröhlich J 2018 *Buoyancy Effects on Turbulent Heat Transfer Behind a Backward-Facing Step in LiquidMetal Flow* (Springer International Publishing)

[15] Niemann M and Fröhlich J 2017 *Flow Turbul. Combust.* **99** 705–728

[16] Jaeger W *et al.* 2017 *IOP Conf. Ser. Mater. Sci. Eng* **228**

[17] Schumm T, Frohnapfel B and Marocco L 2016 *J. of Phys.: Conf. Series* **745** 032051

[18] Schumm T, Frohnapfel B and Marocco L 2017 *Heat Mass Transf* 1–11

[19] Manservisi S and Menghini F 2016 *Nucl. Eng. Des.* **273** 251–270

[20] Manservisi S and Menghini F 2015 *Nucl. Eng. Des.* **295** 251–260

[21] Pacio J *et al.* 2015 *Nucl. Eng. Des.* **290** 27–39

[22] Launder B and Sharma B 1974 *Letters in Heat and Mass Transfer* **1** 131 – 137

[23] M Kays W 1994 *J. Heat Transfer* **116** 284–295

[24] Sobolev V 2011 Database of thermophysical properties of liquid metal coolants for GEN-IV